# High-Resolution Double-Quantum $^{31}$P NMR: A New Approach to Structural Studies of Thiophosphates

**Jörn Schmedt auf der Günne and Hellmut Eckert***

*Dedicated to Professor Bernt Krebs on the occasion of his 60th birthday*

**Abstract:** High-resolution double-quantum $^{31}$P NMR spectroscopy was used to provide structural information about crystalline and glassy thiophosphates. Double-quantum coherences are created under MAS conditions by phase-modulated continuous-wave irradiation such that the nutational frequency is a multiple of seven rotor periods (C7 sequence), and the intensity of the double-quantum coherence is measured as a function of the excitation time. As demonstrated with reference compounds, the double-quantum excitation dynamics determined in this fashion differentiate clearly between orthothiophosphate ($PS_4^{3-}$), pyrothiophosphate ($P_2S_7^{4-}$) and hexahypothiophosphate ($P_2S_6^{4-}$) units based on differences in the strength of $^{31}$P homonuclear dipole–dipole couplings. By means of this method, a structural model is presented for the crystallization of glassy $Li_4P_2S_7$.

**Keywords:** magic-angle spinning · NMR spectroscopy · phosphorus · sulfur · thiophosphate

## Introduction

Binary and ternary sulfides and selenides based on elements of main group 13–15 are of considerable interest in solid-state chemistry owing to the richness in structural features in the crystalline state.[1–4] In addition, many of these are systems for glasses with extremely high ionic mobilities, giving rise to interesting applications in the solid electrolyte industry.[5–8] Specifically, the synthetic and structural chemistry of metal thiophosphate systems has been an area of intense research activity.[3, 4] Polychalcogenide flux chemistry has been used in recent years to prepare new ternary and quaternary thiophosphates.[2] The complexity of the equilibria present in such fluxes may also account for the large structural differences between various crystalline and glassy thiophosphates.[9–11] This rather uncommon feature is of considerable interest for a fundamental understanding of glass formation in chalcogenide systems.

Because of the absence of long-range periodicity, only very limited information about the glassy state is available from diffraction methods. In contrast, solid-state nuclear magnetic resonance (NMR) spectroscopy has proven to be an element-selective, inherently quantitative technique uniquely suited for the structural analysis of glasses.[12–14] In particular magic-angle spinning (MAS) allows for a facile quantitative distinction of different local environments based on differences in the corresponding isotropic chemical shifts. This concept has been successfully applied to the characterization of the local order in many glass systems. In particular, the excellent resolution of $^{31}$P MAS-NMR has been used to great advantage for deriving very detailed structural models in a variety of phosphate glasses.[15–18]

Compared with the situation in oxidic glasses, the chemical shift distinction of structural fragments in sulfide-based glasses is much less straightforward. Scheme 1 shows three common structural units present in many thiophosphates. The $^{31}$P chemical shift ranges of these species show considerable overlap, as previously demonstrated for the binary systems $Li_2S-P_2S_5$ and $Ag_2S-P_2S_5$.[7, 8] The structural interpretation of $^{31}$P MAS-NMR spectra of glassy thiophosphates therefore meets with uncertainty, requiring the use of alternative and complementary NMR strategies. Powerful new techniques have recently been developed which reintroduce homonu-

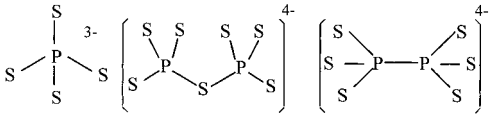


$Li_7PS_6$ $Ag_7P_3S_{11}$ $Hg_2P_2S_7$ $Ag_7P_3S_{11}$ $Hg_2P_2S_6$ $Sn_{1.008}P_2S_6$

Scheme 1. Structural fragments present in crystalline thiophosphate compounds.

[*] Prof. H. Eckert, J. Schmedt auf der Günne
Institut für Physikalische Chemie
Westfälische Wilhelms Universität Münster
Schlossplatz 7, D-48149 Münster (Germany)
Fax: (+49) 251-83-29159
E-mail: eckerth@uni-muenster.de



0947-6539/98/0409-1762 $ 17.50+.50/0

clear dipole–dipole couplings into the high-resolution MAS experiment, providing site-resolved information on internuclear spatial proximity and connectivity in solids.[19–25] Within the scope of these studies, the published $^{31}$P double-quantum NMR results obtained on various crystalline phosphates demonstrate considerable potential for applications to glassy materials.[26–30] In the present contribution, we report how this method can be used to differentiate between common thiophosphate structural units (Scheme 1) and to characterize structural changes encountered when thiophosphate glasses are brought to crystallization.

**Principles and NMR methodology**: Numerous experimental approaches have been used to reintroduce homonuclear dipole–dipole couplings into the magic-angle spinning NMR experiment.[19–24] While the relative merits and drawbacks of these techniques depend greatly on the system studied, a concern common to all real-world applications is the sensitivity to resonance offset and molecular orientation effects. With respect to this issue, a pulse sequence known as C7 has performed well in systems with moderate chemical shift dispersion.[24] The pulse sequence is shown in Figure 1.

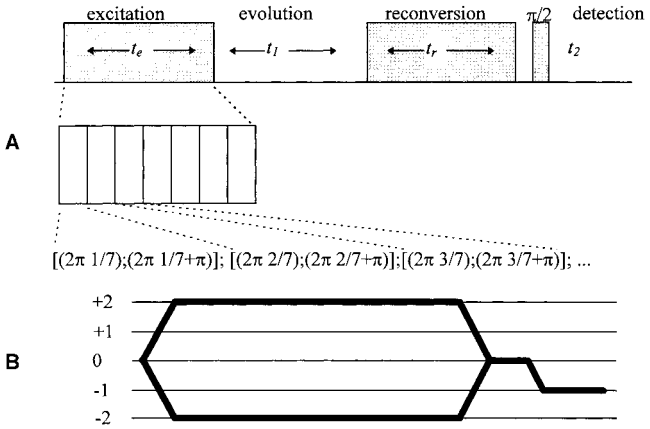


Figure 1. A) Pulse sequence for double-quantum NMR spectroscopy using C7 for excitation and reconversion; B) coherence transfer diagram reflecting the pathways selected through phase cycling.

The sandwich of seven pairs of phase-shifted $2\pi$ pulses per rotor period serves to excite double-quantum (DQ) coherence, which is allowed to evolve for an incremented evolution time $t_1$. The second seven-pulse sandwich serves to reconvert this double-quantum coherence to zero-quantum coherence, and the final 90° pulse creates observable magnetization (single-quantum coherence), which is acquired during the detection period $t_2$. Two-dimensional data processing allows the single-quantum spectrum to be correlated with the double-quantum spectrum, thereby proving the existence of dipole–dipole interactions.

In principle, the strength of the dipole–dipole interaction can be assessed quantitatively by determining the rate at which double-quantum coherence is excited. In such an experiment, the DQ signal intensity is measured under systematic variation of the length of the excitation period. Detailed simulations of the double-quantum coherence excitation dynamics have been presented in the literature for various cases.[24, 29, 31–34] For a static two-spin system, the double-quantum intensity initially increases with increasing excitation time (with a rate dependent on the strength of the dipole–dipole coupling) and then oscillates about an asymptotic value at longer times. Detailed numerical simulations have shown that the average Hamiltonian of the C7 sequence with MAS produces an essentially analogous time-dependent behavior for a two-spin system.[24] In a multispin system, the DQ excitation dynamics are more complicated, and to date calculations have been presented only for static samples.[32, 33] These calculations show a rapid initial increase of DQ intensity at short excitation times, although the oscillatory component never develops. Rather, at longer excitation times the DQ intensity decreases again in an exponential fashion, as higher order coherences are produced. Similar results are expected for the DQ dynamics under the average Hamiltonian of the C7 pulse sequence. As previously reported,[31] a crude approximate description of the DQ dynamics is given by Equation (1). This formula implies that the initial increase

$$I_2(t_e) = A\ t_e^2 \exp\{-t_e/T_2\} \quad (1)$$

of the DQ intensity can be approximated by a series expansion, truncated after the quadratic term. The rate of this initial increase is described by the parameter $A$, which is governed by the second moment describing the strength of the two-spin interaction responsible for the DQ coherence. The constant $T_2$ governing the decay of DQ coherence at longer excitation times reflects the strength of additional spin–spin interactions, contributing to the buildup of higher order coherences. In addition, other relaxation processes, including experimental imperfections,[33, 34] may contribute to this decay. $A$ and $T_2$ can potentially serve as parameters differentiating between the structural fragments shown in Scheme 1. This question will be explored in the present study.

## Experimental Section

**Sample preparation and characterization**: Table 1 gives an overview of the samples investigated. Since some of the starting materials and products are extremely air-sensitive, all preparations and sample manipulations were conducted in a glove box (Vacuum Atmospheres) under an Ar atmosphere. The following starting materials were used: $Li_2S$ (Aldrich, >98%), HgS (Fluka, >98%), P (Aldrich, 99.999%), S (Fluka, 99.999%), SnS (Fluka, 98%), $Ag_2S$ (Fluka, >98%), $P_2S_5$ (Fluka, 98%). Syntheses were carried out within sealed evacuated quartz ampules (pressures $< 10^{-4}$ bar), with the reaction times and temperatures listed in Table 1. Identity and purity of the crystalline materials were ascertained by X-ray powder diffraction (Guinier–Huber, $Cu_{K\alpha}$) and by comparing their solid-state $^{31}$P MAS-NMR spectra with literature data where known. Glassy $Li_4P_2S_7$ was obtained by rapid (ice water) quenching of the melt within a sealed ampule. The completely glassy state was ascertained by the absence of sharp X-ray powder diffraction peaks, and by differential scanning calorimetry with a Netzsch DSC 200 differential scanning calorimeter. At the heating rate of 10 °C min$^{-1}$, a value $T_g = 216$ °C was obtained, in agreement with the literature value.[9]

**Solid-state NMR**: All NMR experiments were carried out at 202.3 MHz on a Bruker DSX 500 NMR spectrometer equipped with a commercial 4 mm MAS-NMR probe. The quality factor of this probe was lowered to 100 by adding a 150 kΩ resistor in parallel to the coil. Samples were rotated within zirconia spinners. By means of appropriate teflon spacers, the sample was

Table 1. Synthesis conditions and structural references for the crystalline materials studied.

| | Starting materials | Experimental conditions | Structural reference |
|---|---|---|---|
| $Hg_2P_2S_6$ (crystalline) | HgS, P, S | 800 °C, 1 d; −10 K h$^{-1}$, 3 d | [37] |
| $Hg_2P_2S_6$ (crystalline) (presumed stoichiometry, impurity in $Hg_2P_2S_7$ preparation) | HgS, P, S(excess) | 240 °C, 1 d | new phase assignment (see text) |
| $Li_4P_2S_6$ (crystalline) | $Li_2S$, P, S | 850 °C, 2 h; 325 °C, 6 d | [10] |
| $Sn_{1.008}P_2S_6$ (crystalline) | SnS, $P_2S_5$ | 800 °C, 1 d; −10 K h$^{-1}$, 3 d | [38] |
| $Hg_2P_2S_7$ (crystalline) | HgS, P, S(excess) | 240 °C, 1 d | [39] |
| $Ag_7P_3S_{11}$ (crystalline) | $Ag_2S$, P, S | 850 °C, 2 h; 500 °C, 2 d | [36] |
| $Li_7PS_6$ (crystalline) | $Li_2S$, P, S | 600 °C, 3 d | [40] |
| $Li_4P_2S_7$ (glassy) | $Li_2S$, P, S | 900 °C, 2 h ice-water, quench | |

confined to the middle 1/3 of the rotor volume. A commercially available pneumatic control unit was used to confine MAS frequency variations to a ±2 Hz interval for the duration of the experiment. Chemical shifts are externally referenced to 85 % phosphoric acid. 2-D correlated spectroscopy (COSY) experiments in the phase-sensitive mode (States-TPPI method)[35] were carried out on $Ag_7P_3S_{11}$, using MAS at a spinning speed of 10 kHz and rotor-synchronized incrementation in the $t_1$ domain (512 experiments). The 90° pulse length was 1.9 μs. 8 scans were added at a recycle delay of 3 s, and an 8-step phase cycle was used.

The shortest excitation time in the double-quantum experiments consists of a continuous-wave block of two rotor periods' length, with 14 different phase entries as previously detailed.[24] In subsequent experiments the number of rotor cycles is successively increased. Phase cycling used during the excitation period and during the acquisition were set to select the coherence pathways shown in Figure 1. All data were acquired with a four-step phase cycle, using the States method for obtaining pure absorption 2-D double-quantum spectra. The rf field strength was optimized for each sample by adjusting the amplifier power on a 2π pulse of fixed length, while the rf field strength of the final read pulse was determined independently. A 2 μs phase preset time for the digital phase shifter was chosen. The evolution time $t_1$ in these 2-D experiments was rotor-synchronized in all experiments. Typical experimental conditions were: spinning speed 10 kHz, recycle delay 1 – 70 s, 128 $t_1$ increments. The most critical parameter for the success of the experiment is the length of the spin-lattice relaxation time, which in most of the samples lies in the vicinity of several minutes.

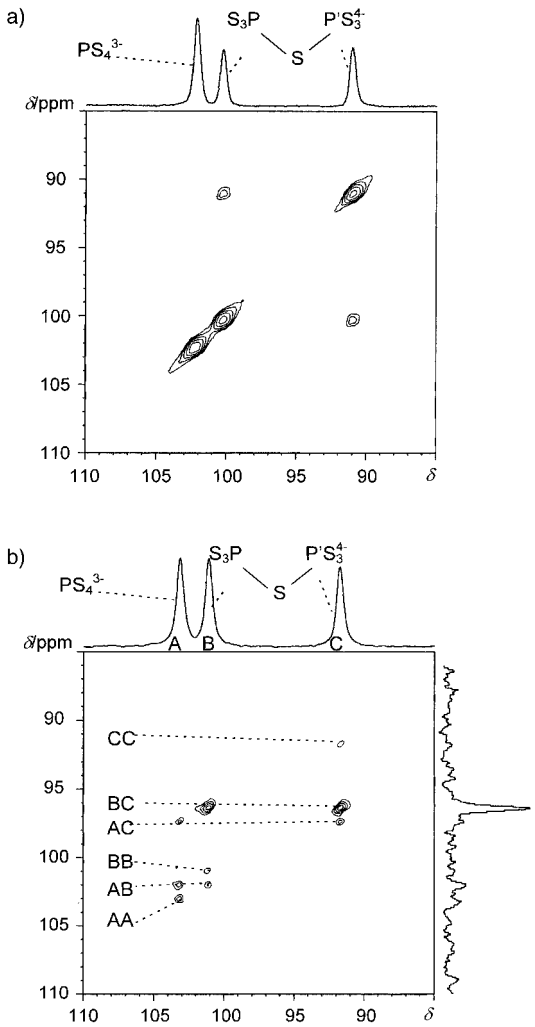


Figure 2. a) 2-D correlated spectrum (COSY) of $Ag_7P_3S_{11}$, symmetrized data in magnitude; each contour level reflects a 2.5-fold gain in intensity, S/N = 770, one pulse spectrum acquired with a relaxation delay of 1 s. b) 2-D double-quantum spectrum of $Ag_7P_3S_{11}$. The P – S – P connectivity is clearly identified by the intense crosspeak B – C in the double-quantum dimension.

## Results and Discussion

The crystalline materials investigated were chosen as prototype compounds representing each of the structural fragments depicted in Scheme 1. In the case of $Ag_7P_3S_{11}$, the $^{31}$P MAS-NMR spectrum contains three resonances belonging to the isolated $PS_4^{3-}$ and the two inequivalent atoms of the thiopyrophosphate ($P_2S_7^{4-}$) groups. Figure 2a illustrates the assignment of these resonances based on a COSY experiment. The intense cross-correlation peaks between the resonances at 101.1 and 91.1 ppm indicates coherence transfer between these spins due to scalar spin – spin interactions revealing the P – S – P connectivity. Figure 2b shows the 2-D correlation spectrum of this compound, obtained by the C7 sequence. Note the strong double-quantum transition (BC) obtained between the two phosphorus sites of the $P_2S_7^{4-}$ group. In addition, weak double-quantum auto- and cross-correlation peaks are also observed in this spectrum, because of weaker long-range dipole – dipole interactions.

Figure 3 shows the experimental results obtained by applying the C7 sequence to the crystalline compounds under investigation where the excitation period is systematically incremented. In the absence of absolute intensity measurements, the data presented here are internally normalized. As described in the previous section, the intensity of the double-quantum coherence at first increases as a function of $t_e$, while at long excitation periods a subsequent decrease is observed. Most importantly, Figure 3 illustrates that the double-quantum dynamics can clearly differentiate between the three types of structural fragments present in these model compounds. Figure 4 shows a typical fit to Equation (1), resulting in the fitting parameters $A$ and $T_2$. As illustrated in Table 2, both the parameters A and $T_2$ provide an unambiguous distinction between the structural fragments represented by these model compounds. As discussed above, the parameter $A$ is expected to depend on the dipolar second moment characterizing the dipolar coupling between the two closest spins in the sample. While Table 2 reveals a correlation, a more detailed discussion of this relationship requires absolute



0947-6539/98/0409-1764 $ 17.50+.50/0 *Chem. Eur. J.* **1998**, *4*, No. 9

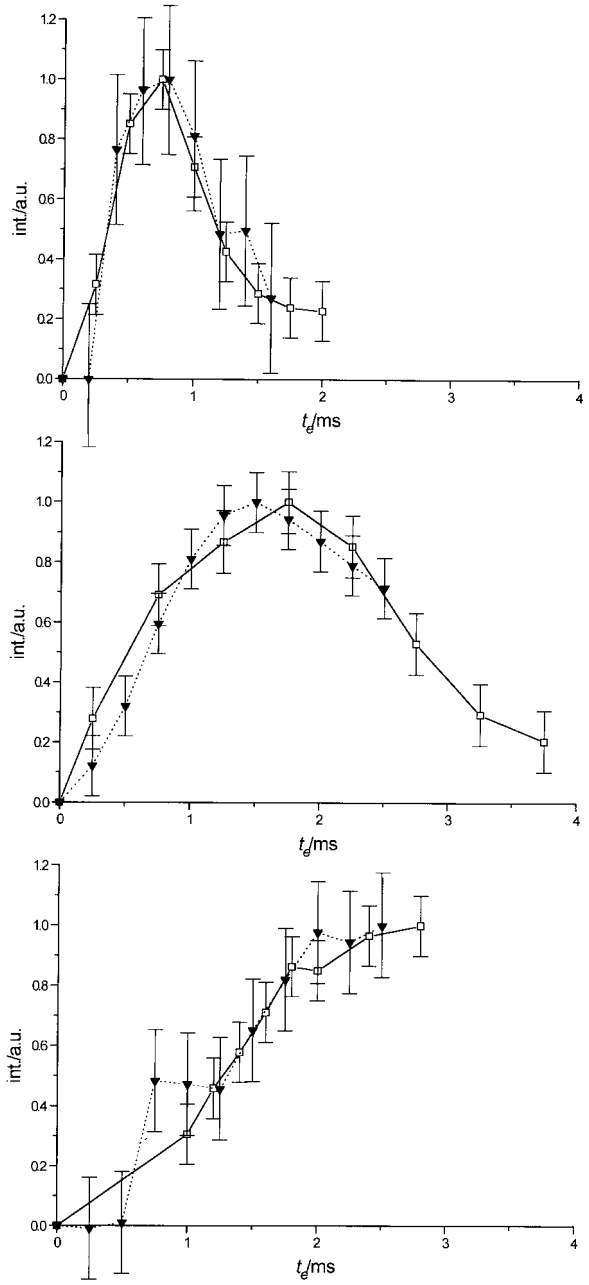


Figure 3. Double-quantum excitation profiles for compounds bearing typical structural fragments in crystalline thiophosphates. Top: $P_2S_6^{4-}$ units in $Sn_{1.008}P_2S_6$ (□) and $Hg_2P_2S_6$ (▼); middle: $P_2S_7^{4-}$ units in $Ag_7P_3S_{11}$ (▼) and $Hg_2P_2S_7$ (□); bottom: $PS_4^{3-}$ units in $Ag_7P_3S_{11}$ (▼) and $Li_7PS_6$ (□). Error bars are estimated from the signal-to-noise ratio.

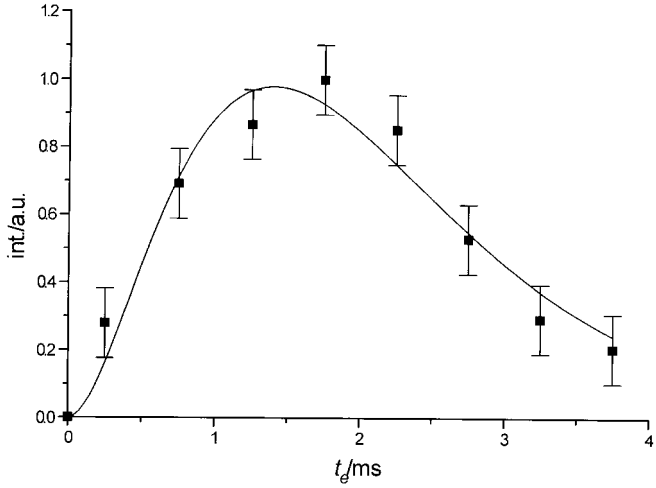


Figure 4. Fit of the double-quantum excitation curve for the compound $Hg_2P_2S_7$ to Equation (1).

DQ intensity measurements and additional studies on a larger number of reference compounds. Such studies are currently being carried out in our laboratory.

In the sample of the $Hg_2P_2S_7$ model compound, a separate resonance was observed at $\delta = 102.6$, indicating the presence of an impurity of unknown structure. The double-quantum excitation profile of this resonance was determined to be very much like that measured for the model compounds with the $P_2S_6^{4-}$ unit (see Table 2). Based on these results, we assign this resonance to a second, previously unknown crystalline modification of $Hg_2P_2S_6$.

Figure 5a shows the $^{31}$P MAS-NMR spectra of glassy $Li_4P_2S_7$ before and after crystallization. As previously reported, this transition is accompanied by a large change in chemical shift.[9] X-ray powder diffraction results have shown that the process can be described by Equation (2). This

$$(Li_4P_2S_7)_{glass} \longrightarrow Li_4P_2S_6 + S \quad (2)$$

produces elemental sulfur and lithium hexahypothiophosphate containing a phosphorus–phosphorus bond.[10] The large $^{31}$P MAS-NMR shift difference encountered in Figure 5a suggests that glassy $Li_4P_2S_7$ has a fundamentally different structure. Based on this result, we previously speculated about the presence of dimeric $P_2S_7^{4-}$ groups. However, the chemical shift offers no definite assignment.

Table 2. Fitting parameters $A$ and $T_2$ from Equation (1), shortest internuclear distance and corresponding dipolar second moment ($M_2(^{31}P-^{31}P)$) calculated from this two-spin interaction for the crystalline model compound and glass samples studied.

| | Model compound | $\delta_{iso}$ ($^{31}$P) | $A$ | $T_2$ [ms] | $r$(shortest P–P) [pm] | $M_2$ ($10^6$ rad$^2$s$^{-2}$) |
|---|---|---|---|---|---|---|
| $PS_4^{3-}$ | $Li_7PS_6$ | 88.5 ± 0.2 | 0.83 ± 0.04 | 1.7 ± 0.1 | structure unknown | – |
| | $Ag_7P_3S_{11}$ | 103.3 ± 0.2 | 0.9 ± 0.1 | 1.5 ± 0.2 | 559 | 0.20 |
| $P_2S_7^{4-}$ | $Hg_2P_2S_7$ | 111.8 ± 0.2 | 1.9 ± 0.1 | 0.70 ± 0.03 | 343 | 1.90 |
| | $Ag_7P_3S_{11}$ | 101.1 ± 0.2; 91.1 ± 0.2 | 1.71 ± 0.04 | 0.77 ± 0.02 | 356 | 1.51 |
| | $Li_4P_2S_7$ (glassy) | 90 ± 1 | 1.5 ± 0.2 | 0.87 ± 0.08 | structure unknown | – |
| $P_2S_6^{4-}$ | $Hg_2P_2S_6$ | 109.4 ± 0.2 | 3.8 ± 0.7 | 0.34 ± 0.05 | 227 | 22.6 |
| | $Hg_2P_2S_6$[a] | 102.6 ± 0.2 | 3.2 ± 0.2 | 0.42 ± 0.02 | structure unknown | – |
| | $Sn_{1.008}P_2S_6$ | 91.3 ± 0.2 (shoulder at 90.6 ± 0.2) | 3.9 ± 0.3 | 0.33 ± 0.02 | 221 | 26.4 |
| | $Li_4P_2S_6$ | 109.1 ± 0.2 (108.5 ± 0.2) | 4.1 ± 0.2 | 0.32 ± 0.01 | – | – |

[a] Presumed stoichiometry of a new compound, structural assignment from NMR behavior (see text).

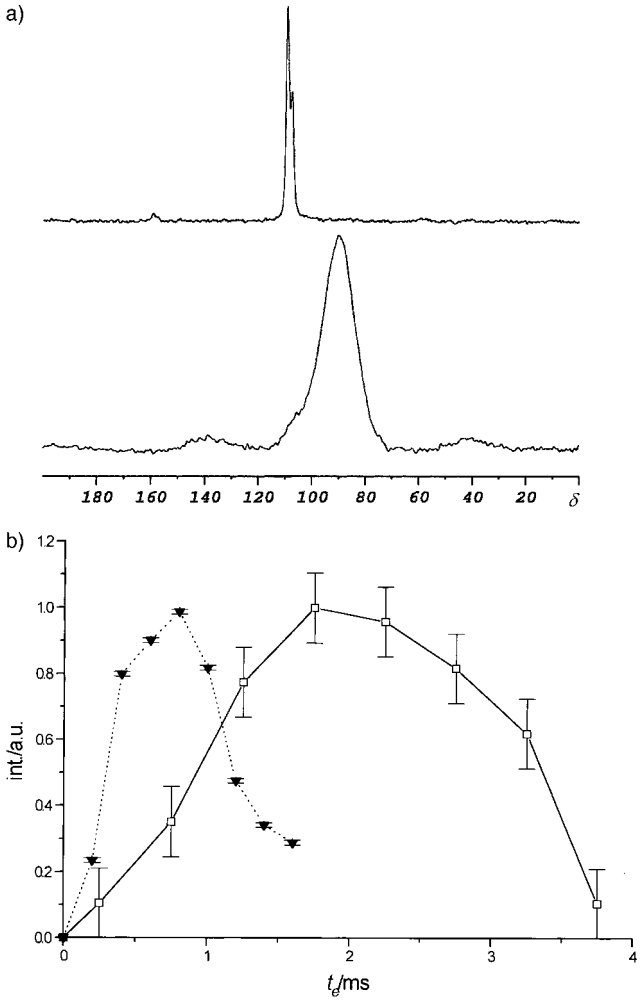


Figure 5. a) 202.3 MHz single pulse $^{31}$P MAS-NMR spectra of glassy $Li_4P_2S_7$ (bottom) and crystalline $Li_4P_2S_6$ (top); b) double-quantum excitation profiles for $^{31}$P atoms in glassy $Li_4P_2S_7$ (□) and crystalline $Li_4P_2S_6$ (▼). Error bars are estimated from the signal-to-noise ratio.

Figure 5b shows the results of the C7 experiments. While the double-quantum excitation dynamics for the crystallized sample closely follow those observed in other hexahypothiophosphates, in the glassy state the typical excitation pattern for a $P_2S_7^{4-}$ group is clearly evident. This result lends strong credence to our previous structural assignment. Evidently, the pyrothiophosphate structure corresponds to an energy minimum only at the local level, and therefore it can be stabilized only in the glassy state. This feature is quite uncommon in the structural chemistry of glass-forming oxides. In contrast, covalent, nonoxidic glasses are frequently characterized by a considerable degree of chemical disorder, including the competition of homo- and hetero-polar bonding, and the existence of striking disparities in the local environments of stoichiometrically analogous crystals and glasses.[12–14]

## Conclusion

The results of the present study reveal the excellent potential of dipolar magic-angle spinning NMR spectroscopy to provide important structural information in crystalline and glassy thiophosphate systems. In particular, the dependence of $^{31}$P double-quantum intensities on the length of the excitation period as measured by the C7 pulse sequence differentiates excellently between typical structural fragments present in such materials. The method can be used to propose structures of previously unknown crystalline compounds and to characterize structural transformations encountered during crystal ↔ glass transitions. Finally, it is clear that the structural chemistry of thio- and selenophosphate systems is much more varied than represented by the fragments shown in Scheme 1. Applications of double-quantum spectroscopy to other types of structural units known in such systems and to a wider range of glassy materials are currently underway.

**Acknowledgments:** We thank Professor H. W. Spiess and I. Schnell (MPI für Polymerforschung, Mainz) for useful discussions and for sharing their experimental results on crystalline phosphates with us prior to publication. Valuable discussions with Professor Christian Jäger (Friedrich Schiller Universität, Jena) are also acknowledged. This research is supported by the Deutsche Forschungsgemeinschaft, grant no. Ec168-1/1, by the Fonds der Chemischen Industrie and by the Wissenschaftsministerium Nordrhein–Westfalen. J.S.a.d.G also thanks the Fonds der Chemischen Industrie for a doctoral stipend.

Received: February 17, 1998 [F1009]

[1] B. Krebs, *Angew. Chem.* **1983**, *95*, 113; *Angew. Chem. Int. Ed. Engl.* **1983**, *22*, 113.
[2] M. Kanatzidis, *Curr. Opin. Solid-State Mater. Sci.* **1997**, *2*, 139.
[3] G. Ouvrard, R. Brec, Rouxel, *J. Mater. Res. Bull.* **1985**, *20*, 1181.
[4] W. Tremel, H. Kleinke,V. Derstroff, C. Reisner, *J. Alloys Comp.* **1995**, *219*, 73
[5] J. P. Malugani, B. Fahys, R. Mercier, G. Robert, J. P. Duchange, S. Buadry, M. Broussely, J. P. Gabano, *Solid State Ionics* **1983**, *9/10*, 659.
[6] J. P. Malugani, G. Robert, *Solid State Ionics* **1980**, *1*, 519.
[7] J. H. Kennedy, Z. Zhang, H. Eckert, *J. Non-Cryst. Solids* **1990**, *123*, 328.
[8] A. Pradel, M. Ribes, *Solid-State Ionics* **1986**, *18/19*, 351.
[9] H. Eckert, Zh. Zhang, J. H. Kennedy, *Chem. Mater.* **1990**, *2*, 273.
[10] R. Mercier, J. P. Malugani, B. Fahys, J. Douglade, G. Robert, *J. Solid-State Chem.* **1982**, *43*, 151.
[11] Zh. Zhang, J. H. Kennedy, H. Eckert, *J. Am. Chem. Soc.* **1992**, *114*, 5775.
[12] H. Eckert, *Prog. NMR Spectrosc.* **1992**, *24*, 159.
[13] H. Eckert, *NMR Basic Princ. Prog.* **1994**, *33*, 125.
[14] H. Eckert, *Angew. Chem. Adv. Mater.* **1989**, *101*, 1763; *Angew. Chem. Int. Ed. Engl. Adv. Mater.* **1989**, *28*, 1723.
[15] R. K. Brow, R. J. Kirkpatrick, G. Turner, *J. Noncryst. Solids* **1990**, *116*, 39.
[16] C. Jäger, M. Feike, R. Born, H. W. Spiess, *J. Noncryst. Solids* **1994**, *180*, 91.
[17] J. W. Zwanziger, K. K. Olsen, S. L. Tagg, *Phys. Rev. B* **1993**, *47*, 14618.
[18] P. Hartmann, J. Vogel, C. Jäger, *Ber. Bunsenges. Phys. Chem.* **1996**, *100*, 1568.
[19] D. P. Raleigh, M. H. Levitt, R. G. Griffin, *Chem. Phys. Lett.* **1988**, *146*, 71.
[20] R. Tycko, G. Dabbagh, *J. Am. Chem. Soc.* **1991**, *113*, 9444.
[21] N. C. Nielsen, H. Bildsoe, H. J. Jakobsen, M. H. Levitt, *J. Chem. Phys.* **1994**, *101*, 1805.
[22] D. M. Gregory, D. J. Mitchell, J. A. Stringer, S. Kiihne, J. C. Shiels, J. Callahan, M. A. Mehta, G. P. Drobny, *Chem. Phys. Lett.* **1995**, *246*, 654.
[23] D. K. Sodickson, M. H. Levitt, S. Vega, R. G. Griffin, *J. Chem. Phys.* **1993**, *98*, 6742.
[24] Y. K. Lee, N. D. Kurur, M. Helmle, O. G. Johannessen, N. C. Nielsen, M. H. Levitt, *Chem Phys. Lett.* **1995**, *242*, 304.
[25] M. Baldus, B. H. Meier, *J. Magn. Reson. A* **1996**, *121*, 65.

[26] W. A. Dollase, M. Feike, H. Förster, T. Schaller, I. Schnell, A. Sebald, S. Steuernagel, *J. Am. Chem. Soc*. **1997,** *119*, 3807.
[27] M. Feike, R. Graf, I. Schnell, C. Jäger, H. W. Spiess, *J. Am. Chem. Soc*. **1996,** *118*, 9631.
[28] M. Feike, D. E. Demco, R. Graf, J. Gottwald, S. Hafner, H. W. Spiess, *J. Magn. Reson. A* **1996**, *122*, 214.
[29] H. Geen, J. Gottwald, R. Graf, I. Schnell, H. W. Spiess, J. J. Titman, *J. Magn. Reson*. **1997**, *125*, 224.
[30] M. Feike, C. Jäger, H. W. Spiess, *J. Noncryst. Solids* **1998**, *223*, 200.
[31] I. Schnell, H. W. Spiess, lecture and poster, GDCh Fachgruppe Magnetische Resonanz, Eichstätt **1996**; personal communication.
[32] M. Munowitz, *Mol Phys.* **1990**, *71*, 959.
[33] A. K. Khitrin, *Phys. Lett.A* **1997**, *228*, 317.
[34] M. Hohwy, H. J. Jakobsen, M. Eden, M. H. Levitt, N. C. Nielsen, *J. Chem. Phys.* **1998**, *108*, 2686.
[35] D. Marion, M. Ikura, R. Tschudin, A. Bax, *J. Magn. Reson*. **1989**, *85*, 393.
[36] P. Toffoli, P. Khodadad, N. Rodier, *Acta Crystallogr*. **1982**, *B38*, 2374.
[37] M. Z. Jandali, G. Eulenberger, H. Hahn, *Z. Anorg. Allg. Chem*. **1978**, *447*, 105
[38] Z. Wang, R. D. Willet, R. A. Laitinen, D. Cleary, *A. Chem. Mater*. **1995**, *7*, 856.
[39] M. Z. Jandali, G. Eulenberger, H. Hahn, *Z. Anorg. Allg. Chem*. **1978**, *445*, 184.
[40] T. Brice, C. R. *Acad. Sci Ser*. **1976**, *C283*, 581.

  0947-6539/98/0409-1767 $ 17.50+.25/0 